

Artificial Neural Network for Investigating the Impact of EMF on Ignition of Flammable Vapors in Gas Stations

Imeh Umoren¹, Saviour Inyang², Ubong E. Etuk³ Aloysius Akpanobong⁴, Gabriel James⁵

¹Department of Cybersecurity, School of Computing and Information Technology, Ikot Abasi, Nigeria

^{2,5}Faculty of Computing and Applied Sciences, Topfaith University, Mkpatak, Nigeria

^{3,4}Department of Computer Science, Akwa Ibom State University, Mkpatak Enin, Nigeria

Email: imehumoren@futia.edu.ng¹, saviour.inyang@topfaith.edu.ng², etuk_ub@yahoo.com³,
 aloysiusakpanobong@aksu.edu.ng⁴, g.james@topfaith.edu.ng⁵

Received: 1 January 2025

Revised: 15 March 2025

Accepted: 22 March 2025

Published: 30 March 2025

Corresponding Author:

Author Name*:

Saviour inyang

Email*:

saviour.inyang@topfaith.edu.ng

DOI: 10.63158/IJAIS.v2i1.19

© 2025 The Authors. This open access article is distributed under a (CC-BY License)



Abstract. The inadvertent ignition of flammable vapors by radio frequency (RF) radiation poses a significant safety risk in mega gas stations, necessitating the development of an intelligent predictive model for hazard prevention. This study proposes Artificial Neural Networks (ANN) Model to classify and predict ignition risks based on structured datasets obtained from smart sensing devices. The model formulation is based on the perceptron architecture, incorporating threshold logic units (TLUs) and multi-layer perceptron's (MLPs) with backpropagation learning for enhanced predictive accuracy. The dataset, preprocessed to remove noise and redundancy, was divided into an 80:20 training-to-testing ratio and evaluated using cross-validation techniques. The experimental results show that the ANN-based model achieved an accuracy of 86%, demonstrating its effectiveness in identifying the impact of hazardous conditions. These findings underscore the robustness of the proposed approach, offering a reliable solution for mitigating ignition hazards in industrial environments. This research contributes to advancing safety protocols by leveraging on machine learning for predictive hazard assessment in flammable vapor-prone areas.

Keywords: Artificial Neural Networks, Radio Frequency Radiation, Flammable Vapors, Perceptron, Machine Learning, Hazard Prediction, Safety in Mega Stations.

1. INTRODUCTION

With the rapid advancement of technology in modern society, electromagnetic radiation has become increasingly prevalent across various environments—including the automotive industry. Numerous vehicle components now rely on electrical energy, and as they transmit electricity through cables and circuits, they naturally emit electromagnetic fields (EMFs). These fields typically operate within frequencies ranging from a few hertz (Hz) to several kilohertz (kHz). This increasing exposure has led to a surge in studies examining the effects of electromagnetic frequency (EMF) on both living organisms and their surroundings.

According to Garaj-Vrhovac et al. [2], Koylu [3], and Lai et al. [4], there are potential positive effects of EMF on biological systems. Conversely, other researchers such as Schüz J. et al. [5], Hook et al. [6], and Lagroye [7] have outlined various negative bioeffects resulting from EMF exposure. Humans are continuously exposed to EMFs from electric transmission lines, telecommunication infrastructures, broadcasting antennas, and satellite communication systems. These sources contribute to the unavoidable presence of electromagnetic radiation (EMR) in our environment. Radio frequency (RF), a major component of EMR, typically ranges from 3 kHz to 300 GHz and can be categorized by its frequency and wavelength as described by Umoren et al. [1].

Typical RF sources include medium and long-wave radios, maritime communication systems, radar systems, wireless networks, amateur radios, FM/VHF/UHF broadcasts, mobile phones, commercial and military transmitters, satellite transmissions, and television stations. Importantly, full electric vehicles, hybrid cars, and electric trains are known to generate stronger EMFs than traditional fuel-powered vehicles [8], [9]. RF radiation can cause metal components to behave like antennas, generating high currents and voltages. This phenomenon can lead to sparking, especially around volatile chemical vapors, which introduces a significant safety hazard.

The introduction of EM flows into electrical detonators can also trigger unintended pyrotechnic ignition. This raises critical concerns about the long-term effects of ELF-EMF and RF-EMF exposure—not just on human health [26] but also on flammable vapor ignition. Notably, brain cells are especially sensitive to ELF fields emitted by mobile

phones due to their proximity to the user's head and the associated specific absorption rate (SAR) [10].

As mobile broadband networks (MBBN) expand rapidly, they present both opportunities and risks for the telecommunications sector. Mobile broadband efficiency measures both qualitative and quantitative aspects of network performance, based on active connection assessments [11]. However, transmitters used in radar, radio, and television systems emit enough electromagnetic energy to induce voltages and currents in conductive materials—such as tanker vessels, pipelines, vent stacks, and metal structures in gas stations.

Despite the vast research on radiation control, no comprehensive study currently exists to assess RF-induced ignition of flammable vapors specifically in gas stations. This highlights the need for a targeted investigation. Understanding the ignition potential from RF radiation in mega stations is vital for improving risk prediction and safety evaluation. For instance, an experiment by Choi [14] tested the effect of EM radiation on a metallic loop within a shielded room. When exposed to a radio transmitter, the highest voltage was recorded at a transmission frequency of 61 MHz.

Further interest in RF-induced ignition is evident in studies such as those by Eckhoff R. K. and Thomassen [15], who examined ignition risks in offshore plants. They found that any device emitting high-frequency energy (10 Hz to 10 GHz) could potentially act as an ignition source under the right conditions—particularly when nearby structures serve as receiving antennas. Their findings emphasize the need for safety protocols informed by such risks. Based on BS 6656:2002 standards, Bradby [16] conducted several practical risk assessments, while other studies [17] have adopted a sequential risk evaluation approach guided by the same code.

Radio frequency radiation can ignite flammable substances through two main mechanisms: High-Frequency Dielectric Heating (HFDEH), which involves direct thermal energy, and Antenna Coupling, which leads to indirect conduction [21]. Existing work [22] has shown that RF radiation can detonate explosives directly or activate electro-explosive devices (EEDs) through such indirect means. However, the specific interactions

between RF radiation and flammable gases remain poorly understood and under-researched.

In Nigeria, regulations governing the siting and operation of petrol and gas stations are administered by the Nigerian Upstream Petroleum Regulatory Commission (NUPRC) [23]. These standards address fire safety, underground storage, wastewater treatment, and licensing, but critically lack provisions for RF-related ignition risks in hazardous environments. This regulatory gap leaves mega stations particularly vulnerable to electromagnetic-induced fire hazards.

This study, therefore, proposes the development of an Artificial Neural Network (ANN) model to assess the impact of electromagnetic radiation on the ignition of flammable vapors in mega gas stations across Nigeria's Niger Delta region. Artificial intelligence (AI) and machine learning (ML) methods enable systems to learn and improve through data analysis [12]. ML has proven effective in identifying hidden data patterns that traditional analysis cannot detect [25], allowing algorithms to refine insights iteratively [13].

The objective of this study is to investigate the role of various factors in unintentional ignition within mega stations. These factors include the strength of the RF signal, the energy contained in the radiation, the function of nearby structures as antennas, absorption rates, ignition pathways, and the presence of combustible gases. By analyzing these parameters, this research seeks to highlight their significance in contributing to RF-induced ignition risks in hazardous environments.

2. METHODS

The schematic in Figure 1 illustrates the methodological framework adopted in this study. This framework underpins the development of a predictive model aimed at preventing the inadvertent ignition of flammable vapors in mega gas stations caused by radio frequency (RF) radiation.

2.1. Model Formulation Using Artificial Neural Network (ANN)

To analyze the potential risk of radio frequency-induced ignition of flammable vapors in mega gas stations, this study employed an Artificial Neural Network (ANN) as the foundational computational model. The ANN was chosen for its ability to recognize complex, nonlinear patterns in data—capabilities that traditional linear models often fail to capture in dynamic, safety-critical environments.

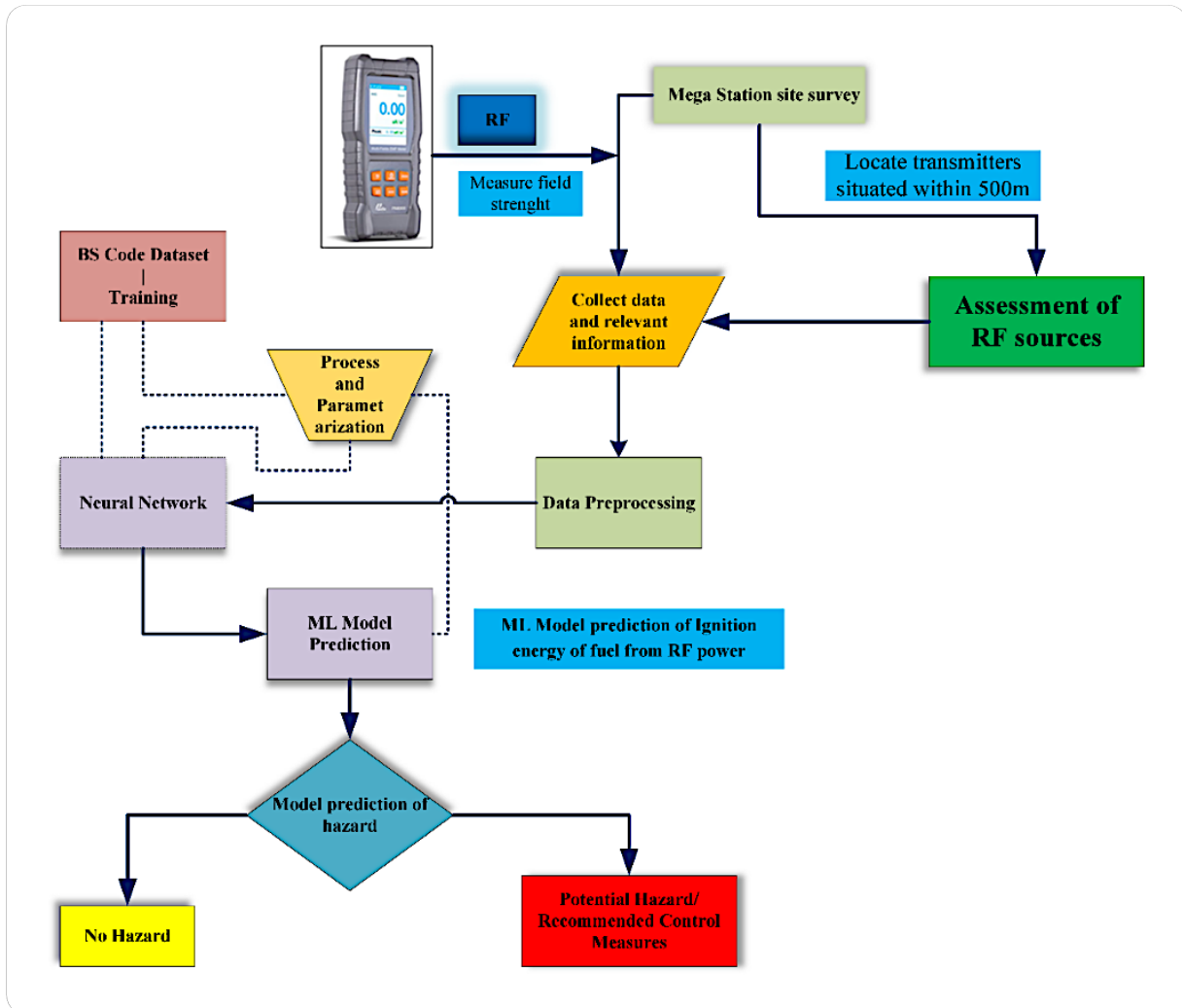


Figure 1. Hybrid Framework for Ignition of Flammable Vapours in Mega Station by RF Radiation

The starting point in ANN design is often the Perceptron, a pioneering neural architecture that mimics the basic decision-making structure of biological neurons. Central to the perceptron is the Threshold Logic Unit (TLU)—also referred to as the Linear Threshold Unit (LTU)—which serves as the computational engine of each artificial neuron. As Geron

A. [18] explains, a TLU processes a set of input signals by computing their weighted sum, comparing this sum to a threshold, and producing a corresponding output signal. Mathematically, the TLU's operation can be represented as shown in Equation 1.

$$z = w_1x_1 + w_2x_2 + \dots + w_nx_n = \mathbf{x}^T \mathbf{w} \quad (1)$$

This equation simply means that each input x_i is multiplied by a corresponding weight w_i , and the resulting products are summed to form a value z . This value represents the neuron's internal state or activation potential. Once this value z is calculated, it is passed through a step function, which acts as a decision gate:

$$h_w(x) = \text{step}(z) \quad (2)$$

Where:

$$z = \mathbf{x}^T \mathbf{w} \quad (3)$$

This function outputs a binary decision: either the neuron "fires" (returns 1) if the input exceeds the threshold, or it stays inactive (returns 0). This simple decision-making model allows the perceptron to act as a linear binary classifier, distinguishing between two classes based on input features.

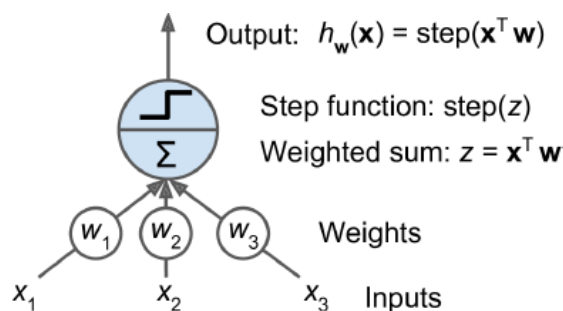


Figure 2. Threshold Logic Unit

In real-world applications—especially those involving multi-class outputs or complex feature patterns—a single TLU isn't sufficient. Therefore, a network of such units, known as a multi-layer perceptron, is employed. The basic perceptron architecture includes an input layer that receives the data, an output layer that returns the final classification, and may include one or more hidden layers for deeper learning. All neurons in a layer are typically fully connected to the neurons in adjacent layers.

This interconnection is clearly illustrated in Figure 3, which shows a perceptron with two input neurons and three output neurons. Such an arrangement enables the model to classify input data into three distinct categories simultaneously, making it a multi-output classifier. To mathematically model these layers and their interconnections, the following equation is used:

$$h_{wb}(X) = \phi(XW + b) \quad (4)$$

Where:

- a) X is the input feature matrix, with each row representing an instance and each column a feature.
- b) W is the weight matrix, containing all weights connecting input neurons to the next layer.
- c) b is the bias vector, allowing the model to shift the activation function for improved flexibility.
- d) ϕ represents the activation function, which could be a step function, sigmoid, or other non-linear functions depending on the desired complexity.

Learning in a perceptron occurs through weight adjustment based on prediction errors. When the output does not match the expected result, the weights are updated to reduce this error using the Perceptron Learning Rule:

$$w_{ij}^{next\ step} = w_{ij} + \eta (y_j - \hat{y}_i) x_i \quad (5)$$

Where:

w_{ij} is there a weight between and the i^{th} input neuron and the j^{th} output neuron

x_i is the i^{th} input for the currently running training instance.

\hat{y}_i is the output of the j^{th} for the current training example's output neuron.

y_i is the intended result of the j^{th} for the current training example's output neuron.

η is the velocity of learning.

This iterative process of forward computation and backward error correction enables the perceptron to "learn" from data. Although the single-layer perceptron is limited to linearly separable problems, it lays the groundwork for more advanced neural networks—capable of tackling non-linear, high-dimensional data, such as that encountered in assessing ignition risks in electromagnetic environments.

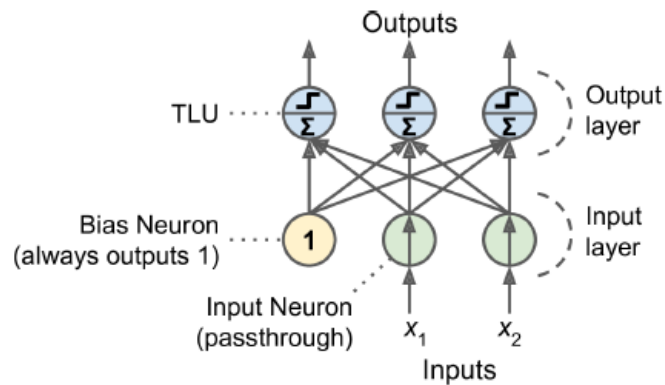


Figure 3. Perceptron Architecture Diagram

2.2. Multi-Layer Perceptron and Backpropagation

The single-layer perceptron modeling mathematical framework can be expanded to include multiple layers. A multi-layer perceptron (MLP), depicted in figure 4, consists of one (pass through) input layer, a number of levels of TLUs known as hidden layers, and one final layer of TLUs known as the output layer. Higher levels are closer to their respective outputs, whereas lower layers are closer to the input layer. Every layer, excluding the output layer, contains a bias neuron that is fully connected to the layer above it. Higher levels are closer to the outputs, whereas lower layers are closest to the input layer. Every layer, excluding the result layer, contains a bias neuron that is fully connected to the layer below it.

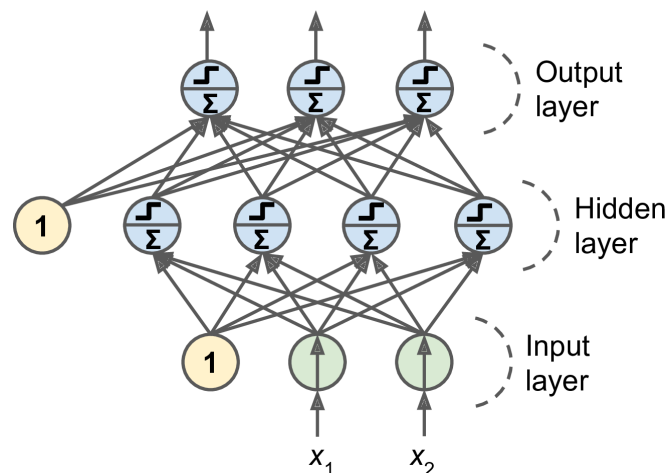


Figure 4. Multi-Layer Perceptron and Backpropagation

The perceptron with multiple layers uses the backpropagation learning method. It merely uses gradient descent as a foundation. This approach employs an effective method for continuously generating the gradients: the backpropagation algorithm can calculate the

gradient of the system's error with respect to each individual model component in a couple of runs through the network (one forward and one backward). In other words, it can determine whether every connection weight and bias term needs to be modified in order to lower inaccuracy. When the network gets these gradients, it just goes through a typical Gradient Descent step and repeats every step unless it merges to the final result. Below are detailed all of the specifics of the artificial neural network that was employed in this research:

- a) It processes the entire training set many times, handling one mini-batch at a time (for instance, having 50 examples each). Epochs are each individual passes.
- b) As a result, each mini-batch is transmitted through the network's input layer, which just sends it on to the top hidden layer. The program then calculates the output for each neuron in this layer (for every single instance in the mini-batch).
- c) The outcome is passed on to the following layer, which calculates its output and does the same, and so on, before we approach the output of the last layer, which is the output layer. The forward pass is just like generating predictions, with the exception that all possible intermediate results are retained because they are necessary for the opposite pass.
- d) The method then calculates the output error of the network (i.e., it compared the system's actual output to its planned output using a loss function and produces a measure of the error).
- e) The error contribution of each output link is then calculated. The chain rule is used analytically to achieve this; it speeds up and improves the process.
- f) After that, when the procedure hits the input layer, the program employs the chain rule to ascertain what percentage of these mistake contributions occurred from every interaction in the layer below. This backwards pass efficiently examines the error gradient over every one of the linking weights in the network by transmitting the error gradient backward through the network.
- g) Applying the error gradient, it just calculated, the procedure then completes a Gradient Descent phase to adjust all of the link weights in the network.

2.3 Model Training and Testing

In the realm of machine learning, the training dataset is the foundational input used to "teach" the model how to perform specific tasks. This dataset serves as the source of knowledge from which the model learns, evolves, and adapts through iterative processing. By leveraging various algorithms and Application Programming Interfaces (APIs), the machine continuously improves its ability to identify patterns, make predictions, and perform intelligent decision-making—all without being explicitly programmed for each individual task.

In essence, machine learning involves constructing algorithms that can interpret large datasets and transform them into actionable insights. These algorithms generate predictions or inferences by developing mathematical representations of the data they ingest. The quality of these inferences heavily depends on the quality of the training data, which must be clean, relevant, and diverse.

For the purpose of this study, the training dataset was generated from real-world statistical field data, collected in accordance with safety and engineering standards. Prior to training, the dataset underwent rigorous pre-processing to eliminate noise, redundancies, and inconsistent values, following the guidance of PD CLC/TR 50427:2004 [19]. This crucial step ensured that the model received high-quality inputs that would enable effective and accurate learning.

The dataset was then partitioned using the widely adopted 80:20 split method—allocating 80% of the data for training purposes and reserving the remaining 20% for testing. The testing dataset, often referred to as an "unseen dataset," is essential for assessing the generalizability, reliability, and precision of the model in real-world applications. Additionally, during the training phase, 20% of the training dataset was set aside as validation data to fine-tune the model's parameters and prevent overfitting. To further enhance the model's robustness and ensure statistical soundness, the study employed a five-fold cross-validation strategy. Under this approach:

- a) The entire dataset was divided into five equal subsets, known as "folds."
- b) In each iteration, four folds were used to train the model, while the fifth fold served as the test set.

- c) This process was repeated five times, ensuring that each fold was used exactly once as a test set.
- d) After completing all iterations, performance metrics such as accuracy, precision, recall, and F1-score were computed to evaluate model consistency and effectiveness across various data partitions [20].

This comprehensive training and validation protocol provided a well-rounded evaluation of the ANN model's ability to generalize across different scenarios and datasets—an essential requirement when dealing with high-risk environments like mega gas stations where the margin for error is minimal. Figure 5 provides a representative cross-section of the training dataset utilized in this study.

	avg_freq	is_Pulse	str_less_than_40m	m_code	multi_tx_factor	EFS	Power	Ignition_Yes
1	0.0750	0.00	0	1.0	1	0.001	1.920000e-07	0
2	0.0170	0.00	0	1.0	1	0.004	3.200000e-07	0
3	0.0450	0.00	0	1.0	1	0.004	1.380000e-06	0
4	0.1000	0.00	0	1.0	1	0.002	7.860000e-07	0
5	0.1300	0.00	0	1.0	1	5.924	1.397901e+01	1
6	0.2165	0.00	0	1.4	1	1.594	2.176042e+00	0
7	0.2165	0.00	1	1.4	1	8.548	6.255599e+01	1
8	0.2165	0.00	0	1.4	2	3.950	1.335868e+01	1
9	0.2165	0.00	1	1.4	2	13.009	1.448918e+02	1
10	0.2165	0.00	0	1.4	2	5.111	2.236452e+01	1
11	0.2165	0.00	1	1.4	2	12.966	1.439363e+02	1
12	0.4050	0.00	0	2.0	2	1.835	7.380093e+00	1
13	0.4050	0.00	1	2.0	2	6.189	8.390980e+01	1
14	0.4700	0.00	0	2.0	2	3.368	3.106736e+01	1
15	0.4700	0.00	1	2.0	2	7.100	1.380240e+02	1

Showing 1 to 15 of 135 entries, 8 total columns

Figure 5. Cross Section of the training dataset

3. RESULTS AND DISCUSSION

3.1. Performance Evaluation

To evaluate the feasibility of using machine learning for hazard prediction, this study implemented an Artificial Neural Network (ANN) to classify and forecast the risk of unintended ignition of flammable vapors caused by radio frequency (RF) radiation. The ANN model was trained on a high-quality, structured dataset acquired from a purpose-built smart device designed specifically for this research. This device collected relevant environmental and electromagnetic parameters across various operational conditions in mega gas stations. To validate the model's performance and reliability, standard

classification evaluation metrics were adopted. The key objective was to determine whether the ANN could accurately identify the presence—or absence—of ignition risks within hazardous environments, thereby enabling proactive mitigation strategies.

One of the primary evaluation tools employed was the confusion matrix, which provides a detailed breakdown of the model's binary classification outcomes. The matrix categorizes predictions into true positives, false positives, true negatives, and false negatives, offering a transparent view of the model's predictive behavior. In this matrix, actual outcomes are listed along the rows, while predicted outcomes are displayed along the columns—enabling a direct comparison between ground truth and model output.

In addition to the confusion matrix, the study leveraged the Receiver Operating Characteristic (ROC) curve, a widely accepted graphical method for evaluating the performance of binary classifiers. The ROC curve plots the true positive rate (recall) against the false positive rate, effectively visualizing the trade-off between sensitivity and specificity. A model with a curve that rises sharply toward the top-left corner is considered highly effective. The false positive rate represents the proportion of actual negatives that were incorrectly classified as positives, and is equivalent to $1 - \text{specificity}$. Therefore, the ROC curve is often interpreted as a plot of sensitivity vs. $1 - \text{specificity}$, giving a comprehensive view of the classifier's robustness under various thresholds.

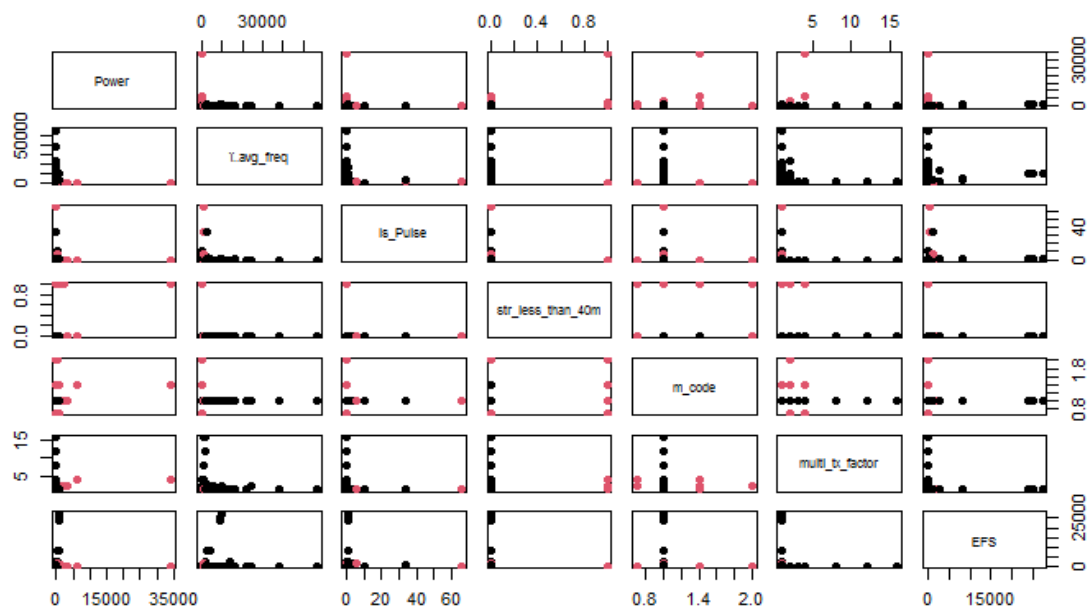


Figure 6. Varied Parameters vs. Power Absorption

To explore how each variable in the dataset correlates with ignition risk, all input features were pairwise-plotted against the power absorption variable—a key indicator of RF intensity. This analysis, visualized in Figure 6, reveals potential nonlinear interactions and offers insight into which variables have the most significant influence on power dynamics and potential ignition thresholds.

A central metric during training is the loss function, which quantifies the gap between the predicted and actual outputs. Unlike accuracy, which simply measures correct predictions, the loss value aggregates all the errors across training or validation instances. It guides the training algorithm by providing gradients used for updating neural weights in the direction of lower error. The total loss across all samples is referred to as the cost, and minimizing this cost is a fundamental goal in optimizing neural networks.

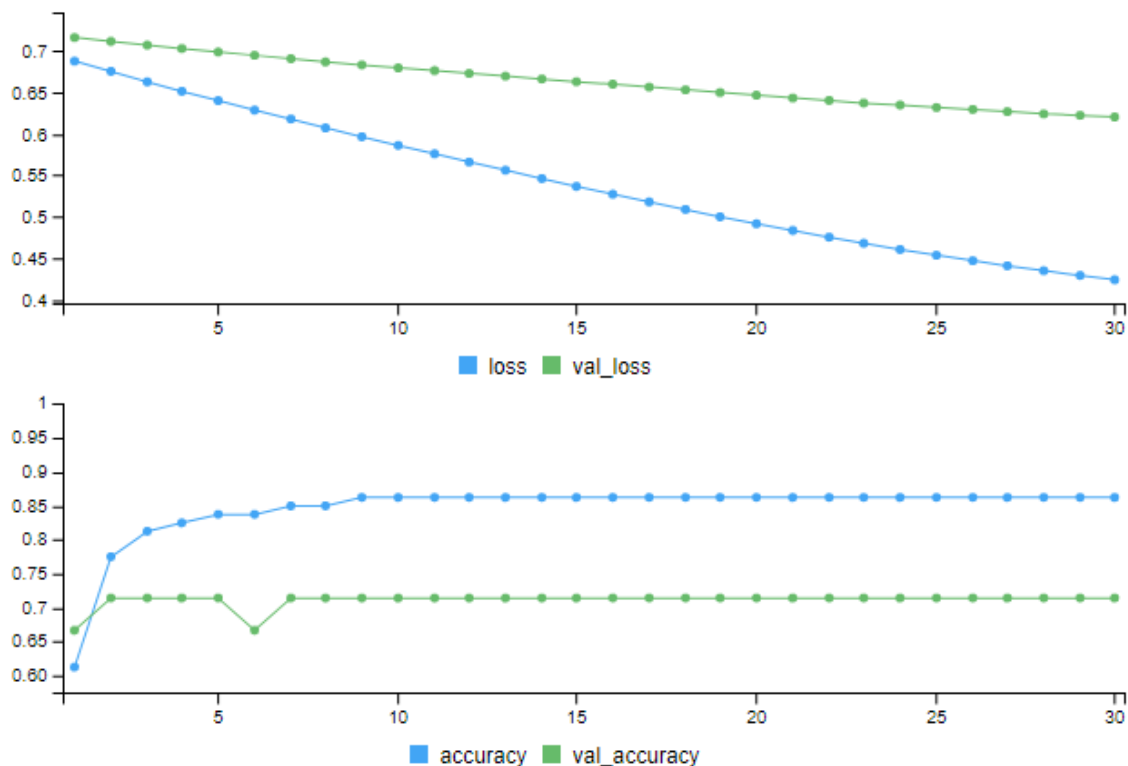


Figure 7. Loss vs. Accuracy Over Training Epochs

As shown in Figure 7, the model's loss consistently declines over successive training epochs, indicating a well-functioning learning process. Notably, both training loss and accuracy improved significantly by the 30th epoch, with loss stabilizing in a downward

trend regardless of the learning method employed. Moreover, Figure 8 illustrates the training and validation performance curves, providing deeper insight into model convergence. The training data shows consistent improvement in accuracy and reduction in loss across the epochs. The validation set, while demonstrating resilience, plateaued around epoch 30—suggesting potential limitations in generalization despite effective training. This behavior underscores the importance of further enhancements in data representation, diversity, and network architecture.

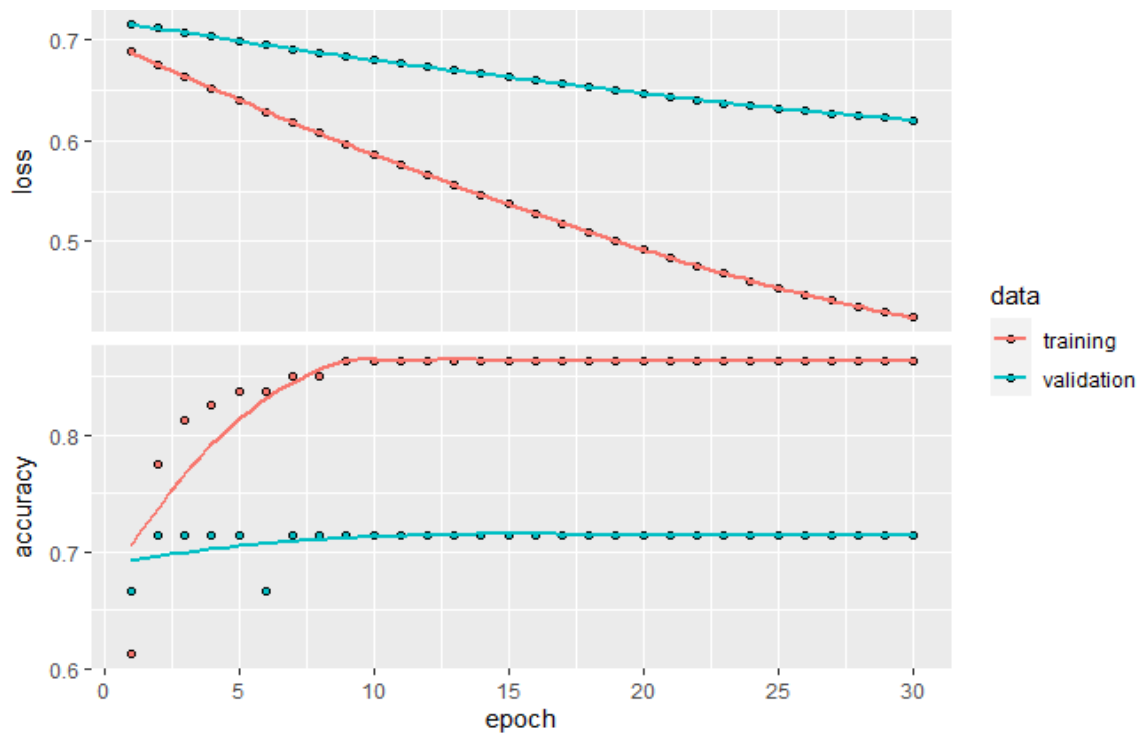


Figure 8. Training and Validation Accuracy vs. Epochs

The concept of epochs is crucial in understanding training dynamics. Each epoch represents a full pass through the training dataset. For large datasets, data is often broken into smaller batches, and a pass of one batch is known as an iteration. If the batch size equals the entire dataset, then one epoch equals one iteration. The model in this study was trained for 30 epochs, with accuracy and loss recorded at each epoch to track learning progress.

A detailed breakdown of training progress is shown in Table 1, which records model performance metrics across all 30 epochs. From the first epoch, the training accuracy

remained stable at 86.25%, while the validation accuracy plateaued at 71.43%, reflecting a consistent training phase but highlighting the need for generalization improvements.

Table 1. Training Iteration Results Over 30 Epochs

Epoch	ETA	Loss	Accuracy	Step Time	Val Loss	Val Accuracy
1	0s	0.4188	0.8625	58ms/step	0.6188	0.7143
5	0s	0.4017	0.8625	25ms/step	0.6126	0.7143
10	0s	0.3850	0.8625	29ms/step	0.6076	0.7143
15	0s	0.3728	0.8625	28ms/step	0.6057	0.7143
20	0s	0.3633	0.8625	26ms/step	0.6047	0.7143
25	0s	0.3556	0.8625	26ms/step	0.6039	0.7143
30	0s	0.3490	0.8625	26ms/step	0.6039	0.7143

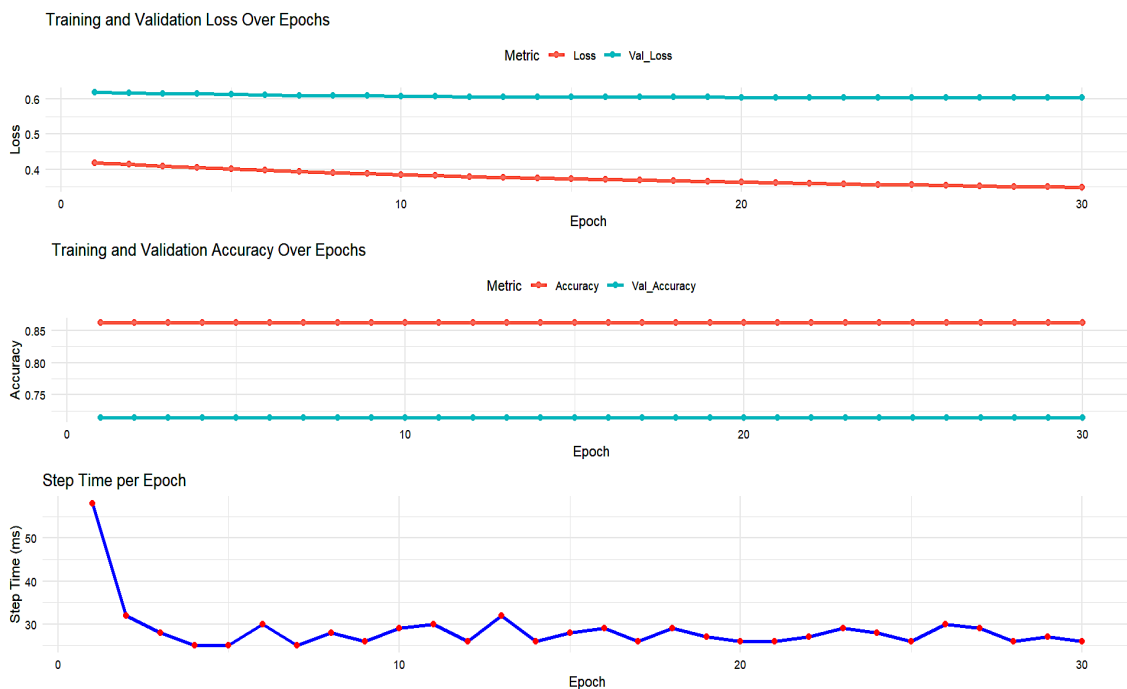


Figure 9. Training and Validation Loss Over Epochs

As visualized in Figure 9, both training and validation losses steadily decreased throughout the 30 epochs. This indicates that the model learned effectively and avoided major overfitting issues, as evidenced by the relatively narrow gap between the two loss curves. However, the static validation accuracy (71.43%) suggests limited generalization capability. This may be due to several factors such as:

- a) Inadequate training data volume or diversity,
- b) Overfitting to the training dataset,
- c) Suboptimal learning rates,
- d) Model reaching a local minimum,
- e) Or lack of regularization techniques.

The step time per epoch, initially variable, stabilized as the model adapted—demonstrating increased computational efficiency with each pass through the dataset. In conclusion, while the ANN model demonstrates high training accuracy and efficient learning behaviour, its generalization remains a challenge. Future research should explore enhancements like data augmentation, architecture refinement, hyperparameter tuning, and regularization strategies to improve real-world prediction performance in complex, high-risk environments such as mega gas stations.

3.2. Discussion

This section critically analyzes and synthesizes the outcomes of the Artificial Neural Network (ANN) model developed to predict the risk of flammable vapor ignition triggered by radio frequency (RF) radiation in mega gas stations. Through an in-depth examination of performance metrics—including accuracy trends, loss curves, the Receiver Operating Characteristic (ROC) curve, and confusion matrix—the discussion provides a holistic understanding of the model's strengths, limitations, and potential for real-world deployment.

From a performance standpoint, the ANN displayed robust learning capabilities. As shown in Figures 7 and 9, the training and validation loss steadily decreased over 30 epochs, indicating successful optimization of the model's internal parameters. This continuous reduction in error signals that the model effectively captured and internalized patterns present in the training data. The high training accuracy of 86.25% further supports the claim that the ANN was able to learn meaningful relationships between features associated with ignition risk scenarios.

However, a closer inspection reveals limitations in the model's generalization capacity. The validation accuracy, which plateaued at 71.43%, did not mirror the improvements seen in training accuracy. This performance gap suggests that the model, while fitting well to

the training data, struggled to extrapolate its predictions effectively to new, unseen data. Such a disparity is often a sign of overfitting or insufficient data variability. It may also indicate that the current ANN architecture lacks the complexity or adaptability required to generalize across diverse operational conditions typical of real-world mega gas stations.

Supporting this interpretation, the confusion matrix and ROC curve further highlight the challenges in classification accuracy. While the model achieved a commendable true positive rate, the presence of false negatives—cases where ignition risk was not detected despite its presence—raises serious concerns in safety-critical environments. False positives are also problematic, though less catastrophic, as they may lead to unnecessary alarms or operational inefficiencies. The ROC curve's moderate performance underscores the need to fine-tune the model for better sensitivity and specificity before it can be considered reliable for field application.

In addition to classification analysis, an exploratory examination was conducted to understand the interaction between various input features and power absorption—a proxy indicator for RF radiation intensity. As illustrated in Figure 6, pairwise feature comparisons revealed several complex and potentially nonlinear relationships. These findings validate the use of an ANN, which, unlike linear models, is inherently capable of modeling such intricate dependencies through its multilayered and nonlinear structure.

Despite the encouraging results, several key limitations emerged. First, the dataset—although meticulously structured and pre-processed—may not encompass the full spectrum of operational and environmental conditions encountered in actual mega stations. This lack of data diversity limits the model's ability to generalize across real-world use cases. Second, the ANN's current architecture may not possess sufficient depth or flexibility to fully capture high-dimensional, contextual variations in ignition risk behavior. Lastly, suboptimal hyperparameters—such as fixed learning rates, insufficient regularization, or limited batch sizes—could be constraining the model's ability to evolve beyond local minima during training.

Synthesizing these findings, it becomes clear that while the ANN framework is technically sound, its practical effectiveness hinges on addressing the noted constraints.

Enhancements in data volume and variability, architectural complexity (e.g., deeper networks or hybrid models like CNN-LSTM), and refined hyperparameter tuning are recommended for future research. Techniques such as dropout, batch normalization, and L2 regularization may also help combat overfitting and improve generalization.

Notably, the model's consistent reduction in training time per epoch demonstrates strong computational efficiency. This trait makes the ANN a promising candidate for real-time applications in embedded systems, particularly in gas stations where immediate hazard detection is critical. However, this potential can only be realized if the model's predictive performance in validation scenarios is improved.

The analysis underscores both the promise and limitations of using ANN models for RF-induced ignition risk assessment. While the current model shows clear technical feasibility and learning efficacy, it falls short in terms of reliable generalization—a key requirement for high-risk safety systems. Future iterations must focus on broader data collection, architectural advancements, and rigorous tuning to create a model that not only learns effectively but also performs reliably in diverse, real-world conditions. With such refinements, the model could evolve into a powerful tool for proactive hazard prevention in flammable environments.

4. CONCLUSION

Radio Frequency (RF) fields are recognized ignition sources for combustible gases and vapors, capable of triggering electro-explosive devices and causing sparks up to 30 kilometers from the source. In environments like mega gas stations—where RF transmitters and industrial machinery are prevalent—this poses significant safety risks. This study developed an Artificial Neural Network (ANN) model to predict the risk of RF-induced ignition using a structured dataset collected over three months. Leveraging perceptron-based architectures, including TLUs and MLPs with backpropagation, the model achieved 86% accuracy in classifying ignition hazards. These results demonstrate the potential of machine learning in enhancing industrial safety through proactive risk assessment. Future work should aim to optimize the model, expand the dataset, integrate real-time monitoring, and validate the system in operational settings to strengthen hazard mitigation efforts.

REFERENCES

- [1] I. J. Umoren, D. E. Asuquo, O. Gilean, and M. Esang, "Performability of retransmission of loss packets in wireless sensor networks," *Computing. Inf. Sci.*, vol. 12, no. 2, pp. 71–86, 2019.
- [2] V. Garaj-Vrhovac, G. Gajski, and S. Pažanin, "Assessment of cytogenetic damage and oxidative stress in personnel occupationally exposed to the pulsed microwave radiation of marine radar equipment," *Int. J. Hyg. Environ. Health*, vol. 214, no. 1, pp. 59–65, 2011.
- [3] H. Koylu, H. Mollaoglu, F. Ozguner, M. Naziroglu, and N. Delibas, "Melatonin modulates 900 MHz microwave-induced lipid peroxidation changes in rat brain," *Toxicol. Ind. Health*, vol. 22, pp. 211–216, 2006.
- [4] H. Lai and N. P. Singh, "Melatonin and a spin-trap compound block radio-frequency electromagnetic radiation-induced DNA strand breaks in rat brain cells," *Bioelectromagnetics*, vol. 18, no. 6, pp. 446–454, 1997.
- [5] J. Schüz, R. Jacobsen, J. H. Olsen, J. D. Boice Jr, J. K. McLaughlin, and C. Johansen, "Cellular telephone use and cancer risk: update of a nationwide Danish cohort," *J. Natl. Cancer Inst.*, vol. 98, no. 23, pp. 1707–1713, 2006.
- [6] G. J. Hook, D. R. Spitz, and J. E. Simet, "Evaluation of parameters of oxidative stress after in vitro exposure to FMCW- and CDMA-modulated radiofrequency radiation fields," *Radiat. Res.*, vol. 162, no. 5, pp. 497–504, 2004.
- [7] I. Lagroye, G. J. Hook, and B. J. Wettring, "Measurements of alkali-labile DNA damage and protein-DNA cross-links after 2450 MHz microwave and low-dose gamma irradiation in vitro," *Radiat. Res.*, vol. 161, no. 2, pp. 201–214, 2004.
- [8] R. A. Tell and R. Kavet, "Electric and magnetic fields < 100 kHz in electric and gasoline-powered vehicles," *Radiat. Prot. Dosim.*, 2016.
- [9] World Health Organization (WHO), *Environmental Health Criteria Monograph No. 238: Extremely Low Frequency Fields*, 2022. Available: http://www.who.int/peh-emf/publications/elf_ehc/en/. [Accessed: 24-Jan-2022].
- [10] Y. X. Liu et al., "Exposure to 1950-MHz TD-SCDMA electromagnetic fields affects the apoptosis of astrocytes via caspase-3-dependent pathway," *PLoS ONE*, vol. 7, no. 4, e42332, 2012.

- [11] I. J. Umoren and S. J. Inyang, "Methodical performance modelling of mobile broadband networks with soft computing model," *Int. J. Comput. Appl.*, vol. 975, pp. 8887, 2021.
- [12] M. Shahhosseini, G. Hu, and S. V. Archontoulis, "Forecasting corn yield with machine learning ensembles," *arXiv preprint arXiv:09055*, 2020.
- [13] I. Kononenko, "Machine learning for medical diagnosis: History, state of the art and perspective," *J. Artif. Intell. Med.*, vol. 1, pp. 89–109, 2001.
- [14] S. W. Choi and H. M. Kwon, "Characteristics of induced voltage in loop structures from high-frequency radiation antenna," *J. Korean Soc. Saf.*, vol. 29, pp. 49–54, 2014.
- [15] R. K. Eckhoff and O. Thomassen, "Possible sources of ignition of potential explosive gas atmospheres on offshore process installations," *J. Loss Prev. Process Ind.*, vol. 7, pp. 281–294, 1994.
- [16] I. R. Bradby, "Practical experience in radio frequency induced ignition risk assessment for COMAH/DSEAR compliance," *ABB Engineering Services, UK. Symp. Ser.*, no. 154, 2008.
- [17] V. Rajkumar and P. Bhattacharjee, "Risk assessment of RF radiation ignition hazard," in *Proc. Int. Conf. Rel. Infocom Technol. Optim. (ICRITO)*, Noida, India, 2015, pp. 1–3.
- [18] A. Geron, *Hands-on Machine Learning with Scikit-Learn, Keras & TensorFlow, Concepts, Tools and Techniques to Build Intelligent Systems*, 2nd ed. Sebastopol, USA: O'Reilly Media, Inc., 2019.
- [19] PD CLC/TR 50427:2004, *Assessment of inadvertent ignition of flammable atmospheres by radio frequency-radiation – Guide*, ISBN 0 580 45883 0, 2006.
- [20] I. Umoren, O. Abe, G. Ansa, S. Inyang, and I. Umoh, "A new index for intelligent classification of early syndromic of cardiovascular (CVD) diseases based on electrocardiogram (ECG)," *Eur. J. Comput. Sci. Inf. Technol.*, vol. 11, no. 4, pp. 1–2, 2023.
- [21] W. B. Wang, H. L. Jiang, and Y. P. Zhang, "Analysis of radio frequency risks in flammable and explosive environments," *Adv. Mater. Res.*, vol. 1092–1093, pp. 717–721, 2015, Trans Tech Publ.
- [22] US-AE (2011) Department of US Army, Ammunition and Explosives Safety Standards, Pamphlet 385–64, USA.
- [23] O. Nwankwo, M. Edem, J. Muku, C. Ike, and E. Ogionwo, "Achieving safety at sea—discussing the safety programs implemented by the Nigerian Upstream Petroleum Regulatory Commission," in *SPE Nigeria Annual International Conference and Exhibition*, Aug. 2022, p. D021S004R002. SPE.

- [24] S. Inyang and I. Umoren, "Semantic-Based Natural Language Processing for Classification of Infectious Diseases Based on Ecological Factors," *International Journal of Innovative Research in Sciences and Engineering Studies (IJIRSES)*, vol. 3, no. 7, pp. 11-21, 2023.
- [25] A. P. Ekong, A. Etuk, S. Inyang, and M. Ekere-Obong, "Securing against zero-day attacks: A machine learning approach for classification and organizations' perception of its impact," *J. Inf. Syst. Inform.*, vol. 5, no. 3, pp. 1123–1140, 2023.
- [26] I. Umoren, S. J. Inyang, U. E. Etuk, and D. Essien, "A clustering-based artificial intelligence approach for minimizing ionizing radiation exposure in Uyo Metropolis, Nigeria," *INNOVATICS: Innovation in Research of Informatics*, vol. 7, no. 1, 2025.